PERGAMON

Deep-Sea Research II 45 (1998) 2547–2569

DEEP-SEA RESEARCH
PART II

The 1996 Gorda Ridge eruption: geologic mapping, sidescan sonar, and SeaBeam comparison results

William W. Chadwick, Jr[a,*], Robert W. Embley[b], Timothy M. Shank[c]

[a]*Oregon State University, Cooperative Institute for Marine Resources Studies, Hatfield Marine Science Center, Newport, OR 97365, USA*

[b]*National Oceanic and Atmospheric Administration/Pacific Marine Environmental Laboratory, Hatfield Marine Science Center, Newport, OR 97365, USA*

[c]*Institute of Marine and Coastal Sciences, Rutgers University, New Brunswick, NJ 08903, USA*

Received 25 June 1997; accepted 3 September 1997

Abstract

As part of a response effort following the February 1996 T-wave swarm on the North Gorda Ridge, camera tows were conducted at the site in April and discovered that a lava flow had erupted onto the seafloor during the earthquake swarm. The lava flow is located on axis between 42.665° and 42.688°N, just south of the axial high of the ridge segment, near the northern extent of T-wave epicenters, and under the site where a hydrothermal event plume was found 2 weeks after the swarm began. Temperature sensors on the camera sled recorded anomalies up to 0.5°C over and near the new flow, showing that it was still actively cooling. Data from camera tows, remotely operated vehicle (ROV) dives, sidescan sonar imagery, and SeaBeam resurveys show that the new flow is 2.6 km long, 400 m wide, and up to 75 m thick, with a volume of 18×10^6 m^3. We interpret that this flow was erupted during the first half of the T-wave swarm. A combination of T-wave, plume, sidescan, and SeaBeam evidence also suggests that another lava flow (not imaged by camera or ROV) may have erupted ~ 8 km to the south between 42.605° and 42.615°N, where the second half of the T-wave swarm was concentrated. However, this possible second eruption site remains unconfirmed.

1. Introduction

Beginning on 28 February 1996, a swarm of T-wave events (acoustic signals from small submarine earthquakes recorded by underwater hydrophones) signaled the

*Corresponding author. E-mail: chadwick@pmel.noaa.gov.

0967-0645/99/$ – see front matter
PII: S0967-0645(98)00083-6

onset of volcanic seismicity on the North Gorda segment of the Gorda Ridge (Fox et al., 1994; Fox and Dziak, 1998). The T-wave epicenters were distributed between the midpoint at 42.75°N (also the axial high) and the southern end of the segment at 42.45°N (Fig. 1). This T-wave swarm lasted about 3 weeks and had many similarities to another detected in 1993 on the CoAxial segment of the Juan de Fuca Ridge, which was associated with dike intrusion, event plume emission, and a volcanic eruption (Baker, 1995; Dziak et al., 1995; Embley et al., 1995b; Fox et al., 1995; Fox and Dziak, 1998). Due to this similarity, a rapid response cruise was quickly mounted on the *NOAA Ship McArthur*, and the ship reached the site about one week after the onset of the T-wave swarm. The *McArthur* was on site from March 9–12 and conducted CTD casts that located and sampled a large event plume (EP96A) about 10 km in diameter, 1 km thick, and centered at about 42.67°N, 126.80°W (Baker, 1998). This discovery and the previous association of event plumes with volcanic eruptions (Embley et al., 1991, 1995b) made a strong case for further work at the site including acquiring photographic imagery of the seafloor to determine whether or not an eruption had also occurred at North Gorda.

A second rapid-response cruise on the *R/V Wecoma* arrived at the site about two weeks after the end of the T-wave swarm and was on site April 6–15. The *Wecoma* conducted camera tows, additional water column surveys, and deployed a RAFOS float into a second event plume (EP96B) (Embley et al., 1996; Lupton et al., 1998; Baker, 1998). The bottom photography and near-bottom temperature data confirmed that an eruption of lava had indeed occurred on the seafloor directly under the location of the first event plume found by the *McArthur* (Embley et al., 1996). Other response cruises followed later in the summer. The *NOAA Ship Discoverer* (June 11–17 and August 7–8) conducted additional plume surveys, collected SeaBeam multibeam sonar data to compare with surveys before the eruption, and obtained sidescan sonar imagery over the eruption site (Chadwick et al., 1996; Embley et al., 1996; Baker, 1998). The new lava flow was further mapped and sampled by two cruises with remotely operated vehicles (ROVs): the *R/V Laney Chouest* with the *Advanced Tethered Vehicle* (August 27–28) and the *R/V Thompson* with *Jason* (September 15–18) (Embley et al., 1996). Geochemical dating of the lava samples confirm that they were erupted during the T-wave swarm (Rubin et al., 1998).

In this paper, we examine the geologic context of the eruption at North Gorda, then describe the character of the new lava flow and the eruption based on near-bottom observations, and finally constrain the area and volume of the flow from SeaBeam comparisons and discuss the evidence for a possible second eruption site on the segment.

2. Geologic and tectonic context of the eruption

2.1. The tectonic setting of the segment

The recent tectonic history of the Gorda Ridge in the NE Pacific has been affected by ridge re-orientations, spreading rate changes, and intra-plate deformation caused

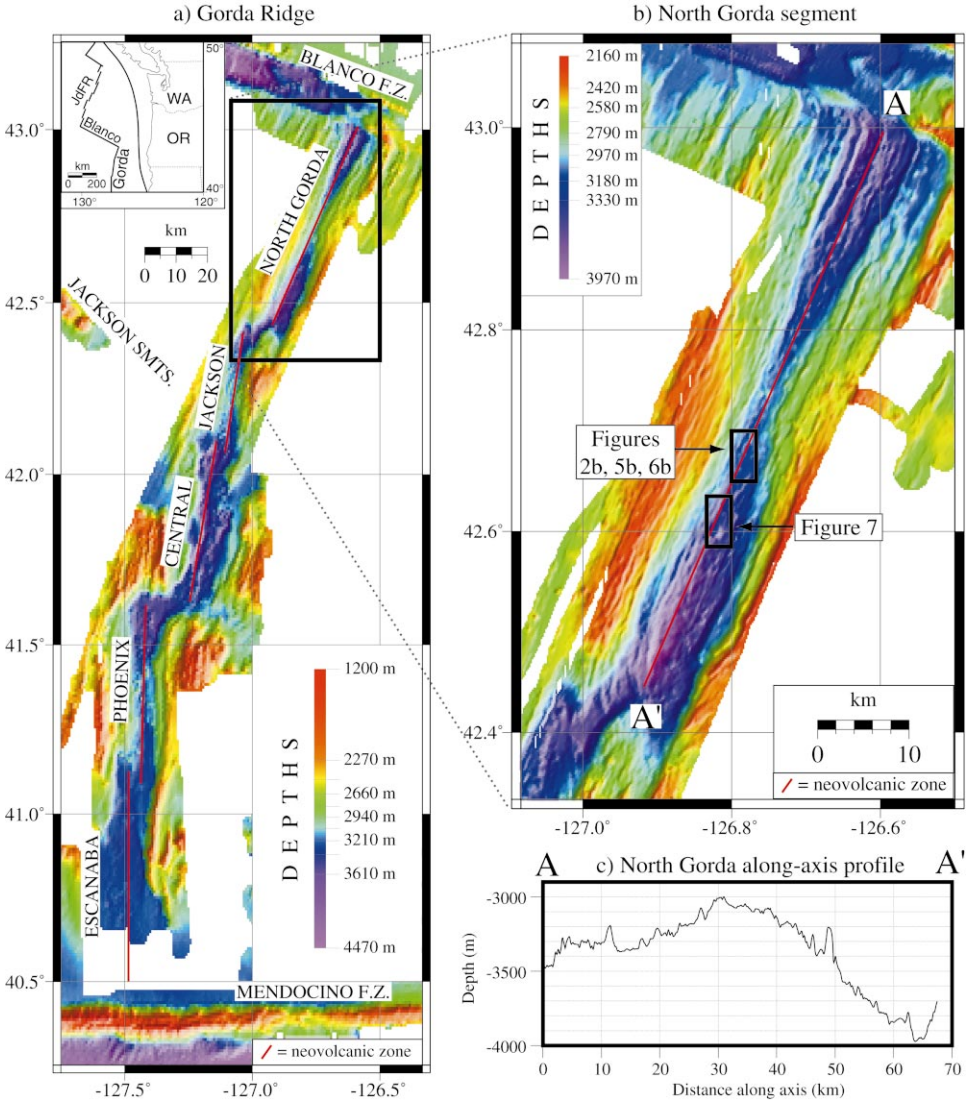

Fig. 1. Location maps showing the setting of the 1996 Gorda eruption. (a) Bathymetry of the whole Gorda Ridge showing the neovolcanic zone along five named segments (red lines). (b) Bathymetry of North Gorda segment showing the hourglass shape of the axial valley. (c) Depth profile of the neovolcanic zone, North Gorda segment, along red line between A and A′ in (b). The 1996 eruption was located just south of the segment axial high.

by interaction with the North American Plate (Wilson, 1986, 1989; Masson et al., 1988). The North Gorda segment is 65 km long and is the northern-most segment on the Gorda Ridge (Fig. 1). Early studies of the Gorda Ridge divided the ridge into three segments (Clague and Holmes, 1987), but more recent ones have identified five, based on offsets of the ridge axis in multibeam bathymetry (Rona et al., 1992). We have assigned names to the segments for clarity in this and future studies (Fig. 1); from north to south: North Gorda, Jackson (named after the adjacent seamounts), Central, Phoenix (named after the ridge west of the segment (Grim et al., 1992)), and Escanaba. The North Gorda segment is bounded on the north by the Blanco Transform Fault Zone and on the south by a non-transform offset with the Jackson segment at $\sim 42.42^{\circ}$N. This southern offset is an obliquely oriented basin, similar to the second-order ridge axis discontinuities described in the south Atlantic which are characterized by both extensional and strike-slip tectonism (Grindlay et al., 1991). The Gorda Ridge spreads at 5.5 cm/yr (full-rate) along the North Gorda segment, but the rate progressively decreases south of this segment to only 2.3 cm/yr (full-rate) at the Escanaba Trough (Riddihough, 1980). Despite the fact that the North Gorda segment spreads at about the same rate as the southern Juan de Fuca Ridge (Tivey, 1994), the two spreading centers are strikingly different in their morphology: the Gorda Ridge has a large rift valley (typical of slow-spreading ridges), whereas the southern Juan de Fuca Ridge has a rifted axial high (typical of fast-spreading ridges). Recent studies have shown that axial morphology at intermediate spreading rates is quite sensitive to small changes in the thermal structure and magma supply beneath the ridge (Phipps Morgan and Chen, 1993). The difference in morphology between Gorda and Juan de Fuca has been explained by slightly thinner crust and slightly cooler mantle temperatures beneath the Gorda Ridge (Hooft and Detrick, 1995). Similar abrupt variations in morphology at constant spreading rate have also been documented on the southern Mid-Atlantic Ridge (Fox et al., 1991) and on the Southeast Indian Ridge (Sempéré et al., 1991, 1996, 1997; Cochran et al., 1997).

Morphologic variations also can occur along strike within a single ridge segment. The axial valley along the North Gorda segment is distinctly hourglass-shaped in map view; the inner valley floor is wide and deep at the segment ends (5–10 km wide; 3500–4000 m deep), and narrow and shallow at its midpoint (2.6 km wide; 3000 m deep) (Fig. 1b). The convex-up depth profile along the segment with the shallowest depths near the segment mid-point is common on other slow to intermediate ridges (Fox et al., 1991; Sempéré et al., 1993, 1997). The peak to trough relief between the axial high and the segment ends is ~ 500 m to the north and ~ 1000 m to the south (Fig. 1c). Within the deep basin at the northern end of the segment (42.9°–43.0°N), a well-developed neovolcanic ridge up to 300 m high is flanked by marginal lows. South of 42.9°N, the rest of the neovolcanic zone is less organized and more diffuse, consisting of discontinuous volcanic constructs of varying shapes and sizes along the axis. A small seamount ~ 140 m high is located at the segment axial high at 42.74°N.

The hourglass shape of the segment in plan view is similar to many ridge segments on the slow-spreading Mid-Atlantic Ridge (Crane and Ballard, 1981; Fox et al., 1991; Sempéré et al., 1993). Sempéré (1993) described two kinds of segment morphology between $24^{\circ}00'$N and $30^{\circ}40'$N on the Mid-Atlantic Ridge – one with narrow,

hourglass valleys with V-shaped profiles, (similar to the North Gorda segment) and the other with wide, deep, U-shaped valleys (similar to the other Gorda segments). On the Mid-Atlantic Ridge, the hourglass segments also have circular mantle Bouguer gravity anomalies centered over the axial highs, which have been interpreted to indicate focused mantle upwelling and/or along-axis variations in crustal thickness (Kuo and Forsyth, 1988; Lin et al., 1990; Fujimoto et al., 1996). Therefore, the V-shaped, hourglass segments are interpreted to be more magmatically robust than the U-shaped segments (Sempéré et al., 1993).

Early studies on the FAMOUS/Narrowgate rift on the Mid-Atlantic Ridge (36°30′N–37°00′N) interpreted the morphology of individual hourglass segments as produced by "extensional wedges" propagating inward from the segment ends in a cyclic tectonic process that transformed narrow rift valleys to wider ones (Ballard and van Andel, 1977; Crane and Ballard, 1981). More recent studies, however, have concluded instead that along-axis variations in the size and depth of the rift valley are steady-state features and can be explained by along-axis changes in magma supply and crustal thickness (Phipps Morgan et al., 1987; Fox et al., 1991; Sempéré et al., 1993, 1997). It is the changing ratio of volcanism to tectonism along the segment that causes the variation in morphology. Dike intrusion and normal faulting are two end-member processes that accommodate extension on a segment in varying proportion, depending on the local magma supply. In areas where magma is available, diking will effectively suppress normal faulting and the topographic relief it creates, because magma pressure often can surpass the least principal stress before the shear strength of the rock is exceeded (Parsons and Thompson, 1991). On the other hand, where the magma supply is low, then faulting will occur more often and will create a deeper and wider axial valley. In this view, the hourglass shape of these segments is due to a variable magma supply along the segment, with a more robust supply near the axial high and a weaker supply toward the segment ends. Thus, the 1996 eruption at North Gorda occurred at the most likely place it could have on the entire Gorda Ridge – near the segment high, on the most magmatically robust and fastest spreading segment on the ridge.

2.2. Previous detailed mapping at North Gorda

Some geologic mapping near the axial high of the North Gorda segment was conducted during the 1980s as part of a survey of hydrothermal activity and mineral resources along the Gorda Ridge. Water column surveys in 1985 detected two plumes along the eastern flank of the rift valley, one at 42.75°N (GR14) and the other at 42.92°N (GR15) (Baker, 1987; Collier and Baker, 1990). In 1985–86, the GR14 site was intensively surveyed and sampled with dredges, towed cameras, and deep-towed sidescan sonar (Rona and Clague, 1989; Clague and Rona, 1990). In 1988, the Navy-operated *SeaCliff* submersible located an active, high-temperature vent field near GR14 at 42.7558°N/126.7087°W, located 2.6 km east of the ridge axis, on the west-facing slope of a fault-bounded bench on the east valley wall, 400 m above the inner valley floor (Rona et al., 1990). No active venting was found on the floor of the axial valley, but bright, white-stained brecciated zones were photographed and

sampled along a small ridge on-axis at 42.758°N, just north of the segment midpoint (Rona and Clague, 1989; Clague and Rona, 1990). Some of the material dredged from this zone was found to consist primarily of high-temperature alteration products, proving that high-temperature fluids had recently passed through the rocks (Howard and Fisk, 1988). Most of the previous near-bottom studies were carried out within ~ 5 km north of the segment axial high, whereas the 1996 eruption began ~ 5 km south of the axial high.

3. Near-bottom observations of the 1996 eruption site

Confirmation that a submarine volcanic eruption has occurred can come only from photographic imagery (or direct observations) of the seafloor. At North Gorda, this was obtained during the *Wecoma* response cruise from a deep-sea camera sled, leased from the Woods Hole Oceanographic Institution. The system included both a Photosea 35 mm film camera and a Benthos digital camera that recorded a grayscale image at 15 s intervals to an internal 2 gigabyte hard drive. The *Wecoma* had only a non-conducting trawl cable available, so the camera system had to be "flown blind" (with no real-time imagery) by measuring its altitude (usually 5–10 m) from a 12 kHz pinger trace on a line scan recorder. The only real-time feedback from the seafloor was through the pinger signal, which was multiplexed to display the relative water temperature from a sensor on the sled. This temperature signal was crude but extremely valuable in finding and mapping the extent of the new lava flow, because the flow was still cooling and the warm water it was venting could easily be detected. Our ability to develop 35 mm film at sea was limited and the digital camera was damaged by over-heated internal components during the first tow, causing the images it recorded to be inaccessible until late in the cruise. Thus, the temperature signal became our main tool to "remotely sense" the new flow while at sea. An internally recording SeaCat CTD also was mounted on the camera frame and provided quantitative temperature and depth data, which were collected on all but one of the camera tows.

We conducted 5 camera tows from *Wecoma*, which collected 7500 film frames and 680 electronic images and covered a cumulative distance of 24 km over ground. The camera tows were centered directly under the area where the *McArthur* had discovered the first megaplume (Fig. 2). The navigation accuracy for the camera tows was about $\pm$ 100 m, since it was estimated using ship navigation, camera depth, and range to the camera. Our first tow (96-1) encountered a temperature anomaly of up to 0.14°C that persisted for 20 min ($\sim$400 m horizontally over ground) with an abrupt onset and rapid return to background. The broad extent of this signal made us suspect its source was a new lava flow, as opposed to isolated point-source or line-source hydrothermal vents. Later examination of the bottom photographs confirmed this interpretation.

The temperature anomalies (short-term elevations in temperature above ambient) frequently coincided with the times that the camera sled was over fresh lava (Fig. 2). At bottom locations coincident with temperature anomaly peaks, yellow hydrothermal staining on the lavas and particles in the water were observed in bottom photographs

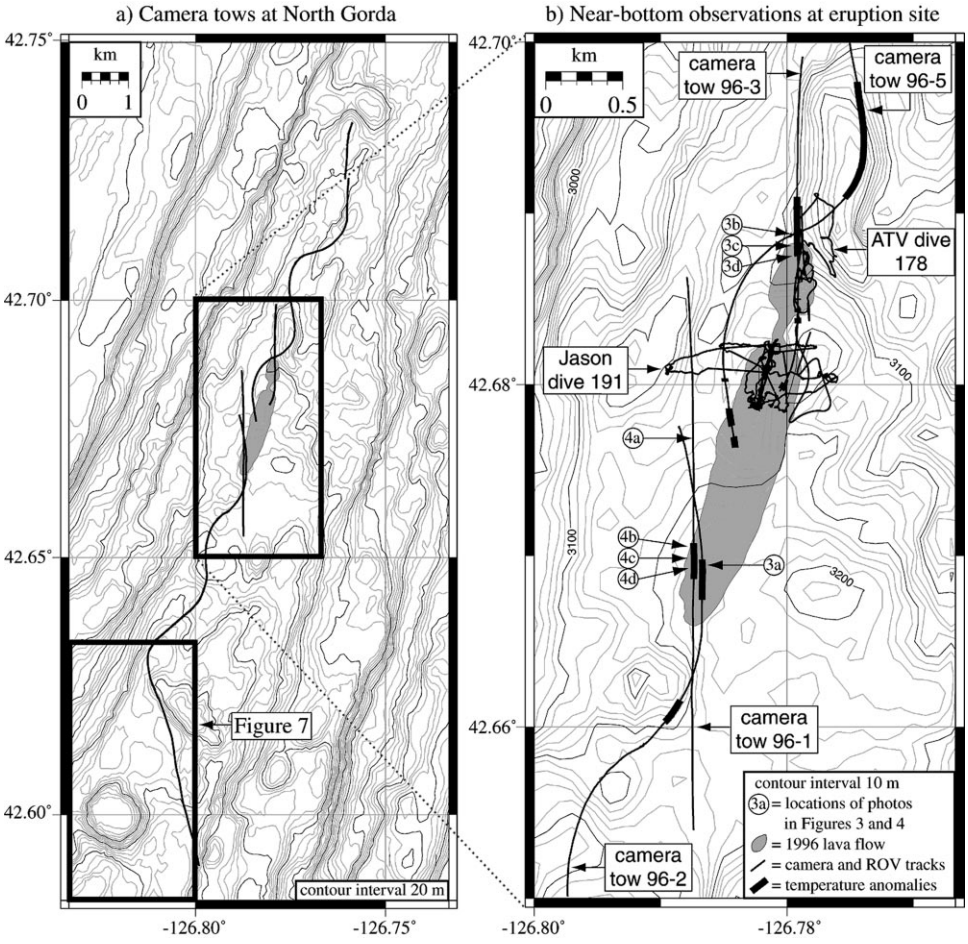

Fig. 2. (a) Post-eruption bathymetry (20 m contours) showing tracks of five camera tows at North Gorda and the location of the 1996 lava flow (gray stipple). Outlines of Figs. 2b and 7 are indicated. (b) Detailed map of 1996 eruption site (10 m contours) showing camera and ROV tracks. Camera tracks are bold where near-bottom temperature anomalies were encountered. Locations of photographs in Figs. 3 and 4 are indicated by circled numbers.

(Figs. 3a and 4d). But at other times, the elevated temperatures were encountered over older terrain and at distances up to hundreds of meters from any known 1996 lava. In fact, the highest temperature anomaly measured (0.5°C above ambient on tow 96-3) was located $\sim$ 75 m north of the 1996 flow over older lava. Temperature anomalies over older terrain were located just north and south of the flow, directly along strike (Fig. 2), suggesting that these signals were related to hydrothermal venting from the dike that fed the 1996 lava flow where it was near the surface. This kind of venting was observed uprift and downrift of the CoAxial lava flow soon after it erupted in 1993 (Embley et al., 1995b; Chadwick and Embley, 1998).

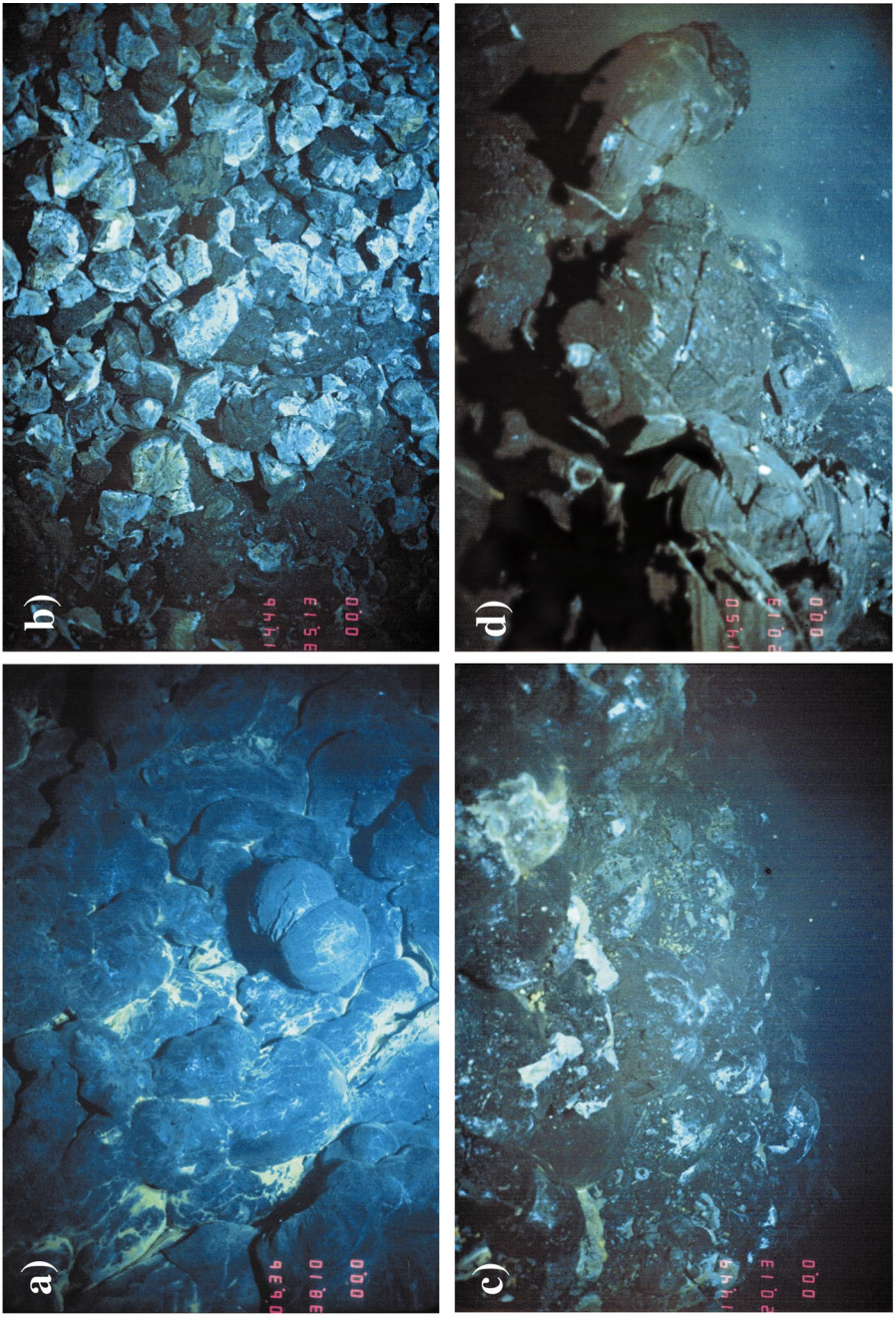
a)
b)
c)
d)

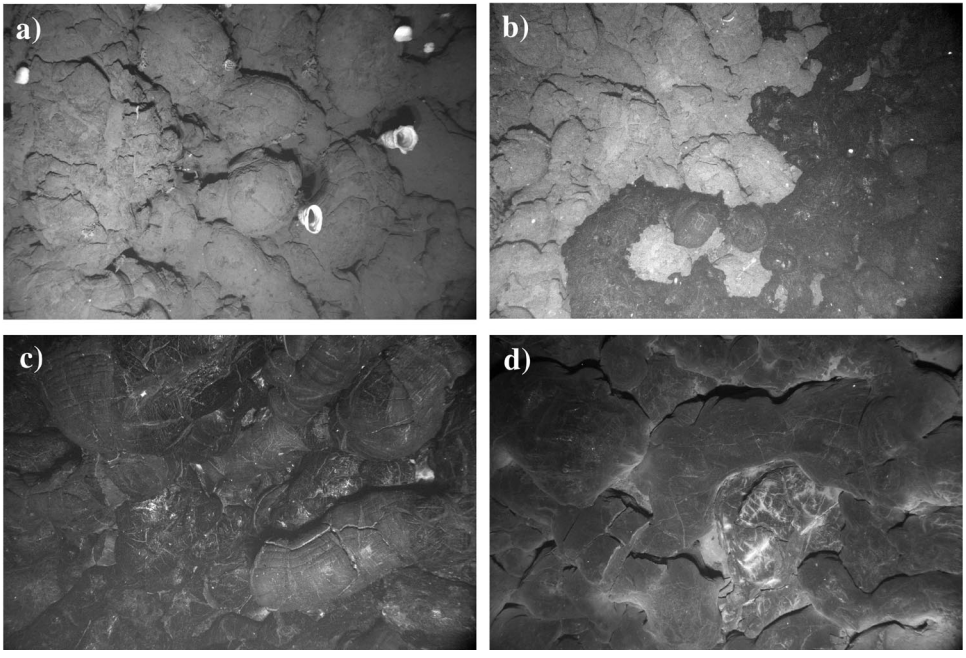

Fig. 4. Grayscale images from the digital camera. (a) Older pillow lavas surrounding the 1996 lava flow with light sediment accumulation and pervasive colonization by non-vent biota (tow 96-1, 17:17:26, field of view ~4 m across). (b) Contact between 1996 lava flow and surrounding older lavas (tow 96-1, 17:57:56, field of view ~6 m across). (c) Dark, glassy striated pillows of 1996 lava flow (tow 96-1, 18:02:26, field of view ~4 m across). (d) Smooth-surfaced pillows with hydrothermal staining where temperature anomaly was measured indicating active venting (tow 96-1, 18:04:11, field of view ~3 m across).

The older lavas surrounding the 1996 flow at North Gorda are dominantly pillow lavas (Fig. 4a), with rare lobate and sheet flows. Sediment cover varies from almost total burial to a thin coating, indicating a wide range of lava ages. The new lava flow is comprised of pillow lavas, and is distinguishable from the surrounding older lavas by its lack of sediment cover (except in areas of hydrothermal venting), its dark and glassy appearance, and by the total lack of biological colonization (Figs. 3 and 4). The older lavas, in contrast, are pervasively ornamented with non-vent biota, including

Fig. 3. Color photographs from camera tows, each with a field of view ~4 m across. (a) Yellow hydrothermal staining on 1996 lava where a temperature anomaly was measured indicating warm water was actively venting out of the flow (tow 96-2, 06:36:38). (b) Talus covered with fine, dark, glassy clastic debris, both probably derived from pillows cascading down the steep northern slope of the 1996 lava flow during its emplacement (tow 96-3, 14:46:35). (c) Near-vertical slope, 80 m high, where many pillows have spalled off the northern edge of the 1996 flow (tow 96-3, 14:49:20). (d) View from the top of the steep slope on the northern edge the 1996 flow showing intact pillow hanging out into space over the cliff below (tow 96-3, 14:50:20).

gorgonaceans (sea fans), stalked and comatulid crinoids, and demospongid and hexactinellid sponges. Throughout our camera surveys, no vent-endemic megafauna was observed. The pillow morphology of the 1996 flow indicates that it was erupted at a relatively low effusion rate of 1–10 m^3/s (Griffiths and Fink, 1992; Gregg and Fink, 1995), which limits the distance lava can flow from an eruptive vent and promotes the emplacement of thick, steep-sided flows.

In fact, the northern end of the 1996 flow is extraordinarily steep and thick. Here the edge of the flow is an almost vertical slope, 80 m high, where pillows are either frozen in place as if pouring out into empty space or were broken off during emplacement (Fig. 3c and d). At the base of this slope there is a thin blanket of glassy clastic debris covering talus (Fig. 3b) and intact older lava up to 150 m north of the new flow, probably derived from the shattering of friable, glassy pillow crusts as they cascaded down the cliff. Camera tow 96-3 happened to recover a sample of the 1996 flow (W9604C3) as it encountered this steep cliff face. This basalt sample was dated by U-series methods, which confirmed that it was erupted near the time of the T-wave swarm (Rubin et al., 1998). The northern part of the 1996 Gorda flow is thicker and has steeper sides than either the 1993 CoAxial flow (Embley et al., 1995b) or the mid-1980s Cleft pillow mounds (Chadwick and Embley, 1994), suggesting that the Gorda lavas were less fluid and erupted at a lower effusion rate and/or with a higher viscosity.

In late August, the U.S. Navy's *Advanced Tethered Vehicle* (*ATV*) visited the site during dive 178 and collected high-resolution video, 7 rock samples, and near-bottom temperature and chemical surveys near the north end of the flow. By this time, venting of warm water from this site had diminished to such an extent that no shimmering water was visible, although temperature anomalies up to 0.4°C were measured (Massoth et al., 1998). In September, dive 191 of the ROV *Jason* was made over the thickest part of the new flow (about 500 m south of the *ATV* dive) and collected high-resolution video, still camera photos, 7 rock samples, made measurements of the magnetic field over the lava, and took several conductive heat flow measurements (Johnson and Hutnak, 1997). On the crest of the flow, thick mats of bacteria and hydrothermal sediment were encountered where Jason measured the highest heat flow. Shimmering water was still visible in a few locations where temperature anomalies up to 1.3°C were measured (H.P. Johnson, pers. comm., 1997). The petrology and geochemistry of the basalt samples recovered from the 1996 lava flow are discussed in Rubin et al. (1998)

4. Sidescan sonar results

In August 1996, an AMS-60 sidescan sonar system, leased from Williamson Assoc. of Seattle and deployed from the *Discoverer*, collected two, 2 km wide swaths over the eruption site. The AMS-60 is towed 150–200 m above the seafloor and sends out acoustic pulses at ~ 60 kHz from each side of the towfish. The amplitude and phase of reflected acoustic energy are then recorded and processed to produce images of the seafloor, which provide a synoptic view and are particularly useful for

highlighting seafloor texture, morphology, and structures. Navigation for the sidescan towfish was estimated from layback calculations.

The sidescan imagery shows that the 1996 flow is one of many hummocky ridges and mounds that make up the ridge axis (Fig. 5). The relatively unfissured neovolcanic zone is 1–2 km wide and is bracketed to the east and west by the extensively faulted axial valley walls. The camera tows show that these ridges and mounds are constructed of relatively young pillow lavas, and the smooth, low-lying areas in between them are heavily sedimented pillow or sheet flows which are considerably older. The pillow ridges and mounds are clearly the most recent volcanic products. Most of the constructional ridges are elongate parallel to the ridge axis, but some are distinctly curved or sinuous and are locally oriented oblique to the ridge axis (Fig. 5). This is

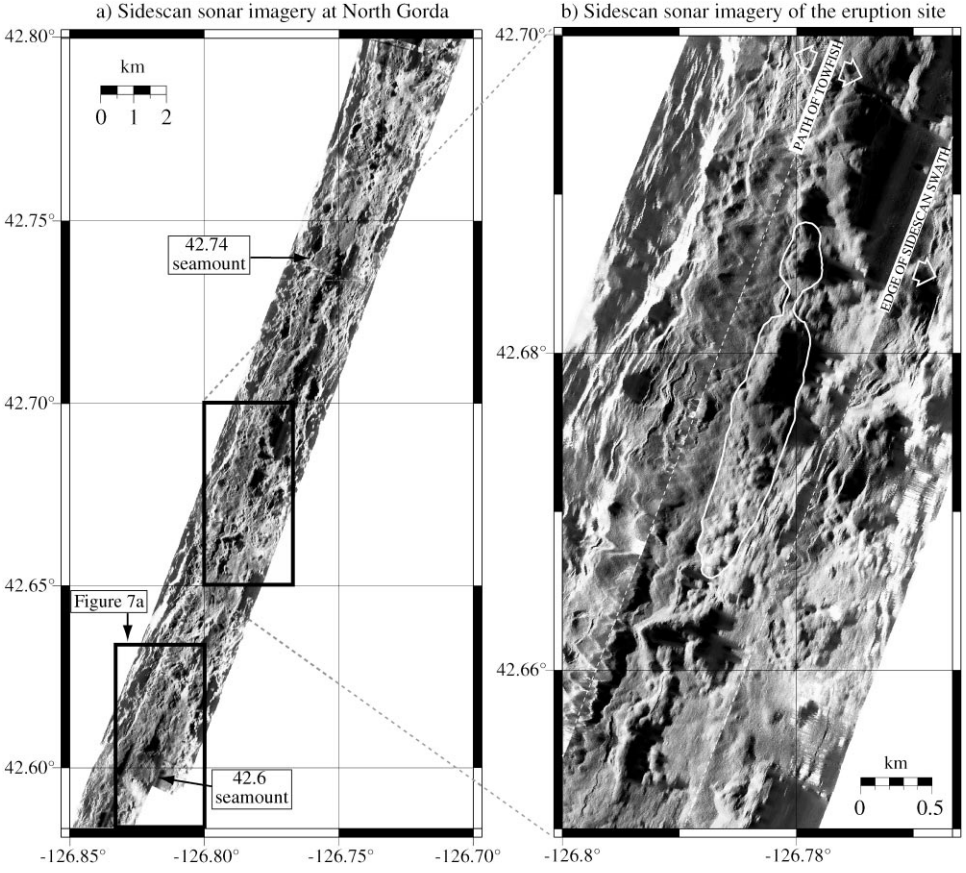

Fig. 5. AMS-60 sidescan sonar imagery at North Gorda (light shades indicate high backscatter, dark shades indicate low backscatter or acoustic shadow). (a) Mosaic of full extent of 1996 sidescan survey, including two, overlapping, 2 km wide swaths. The locations of two on-axis seamounts discussed in the text and the outlines of Figs. 5b and 7a are indicated. (b) Detail of sidescan mosaic showing 1996 lava flow (white outline). Path of towfish and edge of overlapping swath are shown by dashed white lines. White arrows indicate the direction of insonification from the towfish.

unusual since dikes are usually planar and oriented perpendicular to the plate spreading direction at mid-ocean ridges. Rona and Clague (1989) proposed that oblique NW-SE oriented faults along the North Gorda segment help localize hydrothermal venting, and such structures could conceivably channel magma as well. The oblique ridges at North Gorda are either, (1) eruptive products of dikes that intruded at an angle to the ridge axis (produced in one event), or (2) composite constructs of many small, point-source eruptions that coalesce to form a ridge (not produced in one event). We favor the second interpretation, but it is not possible to know the relative importance of these two mechanisms without more detailed mapping and sampling.

There are two seamounts on axis within the sidescan survey, one at 42.6°N/126.823°W and the other at 42.738°N/126.755°W, the latter located at the segment axial high (Figs. 5 and 7). The circular seamounts have diameters of 800–900 m and heights of 150–200 m, and both are mesa-like in that they appear to be capped by relatively smooth, intact, flat-lying lava flows, and their flanks are steep and probably draped with clastic debris. These are similar to flat-topped seamounts described on the northern Mid-Atlantic Ridge (Smith et al., 1995; Head et al., 1996; Smith, 1996). This morphology implies that the seamounts formed over a point-source vent as a stack of radially spreading, cooling-limited flow units which built up a roughly circular edifice, as proposed by Head et al. (1996). The extensive flows covering the tops of the seamounts and their flat-topped shape suggest that the eruption rate remained relatively high until seamount growth ended abruptly (otherwise, they would have a more conical shape).

Although the 1996 flow is obviously young and unfractured in the sidescan imagery, it does not stand out from its surroundings as distinctly new (it could not have been confirmed as new with sidescan alone). The 1996 flow blends in and is just the latest addition to the crust, emplaced with the same eruptive style as many previous events. There are no obvious grabens visible in the sidescan imagery either uprift or downrift of the flow, as has been observed at the Cleft and CoAxial eruption sites and interpreted to have formed during dike intrusion (Chadwick et al., 1996; Chadwick and Embley, 1998). Another striking observation from the sidescan data is that the 1996 flow is very thick in its northern half but quite thin in its southern half. In the northern half, where the pre-eruption SeaBeam bathymetry shows only a relatively flat basin, the sidescan images show a large, steep-sided, hummocky ridge (Fig. 5). This ridge corresponds exactly to the thickest part of the SeaBeam anomaly.

5. Seabeam comparison results

Repeated multibeam surveys after an eruption on the seafloor can be used to quantitatively estimate the location, extent, thickness, area, and volume of new lava flows, if earlier surveys exist and the changes are large enough (Fox et al., 1992). This method has been used to document four recent eruptions on the Cleft segment and CoAxial segment of the Juan de Fuca Ridge (Chadwick et al., 1991, 1995; Fox et al., 1992; Chadwick and Embley, 1994; Embley and Chadwick, 1994; Embley et al.,

1995a). With high-quality surveys, the detection threshold of the multibeam comparison technique is 5–15 m in thickness and 200–300 m in area, making it best suited for detecting eruptions that produce thick accumulations of pillow lava, which are common on the Juan de Fuca and Gorda Ridges.

The first opportunity to collect a repeat SeaBeam survey after the Gorda Ridge eruption was during the summer 1996 cruises on the *Discoverer*. The repeat surveys were GPS-navigated. Unfortunately, the results of the SeaBeam comparisons for the Gorda eruption are less definitive than for previous re-surveys. This is because the original SeaBeam survey over the Gorda Ridge was collected in 1980 and 1981 using Loran-C for navigation, and while this has yielded good results farther north on the Juan de Fuca Ridge, Loran-C navigation is lower in quality on the Gorda Ridge because of poor geometry from the shore-based transmitter stations. The original survey was rigidly shifted to provide a best fit with the 1996 survey, as described in Fox et al. (1992), but internal navigation errors remain as distortions in the original survey. Another (less important) factor that complicates the results is that the repeat SeaBeam surveys were collected during other operations on the *Discoverer* cruises (with non-optimal survey lines and ship speed) due to time constraints. These problems increase the relative noise level in the comparisons—creating more and larger false depth differences—and make it considerably more difficult to discern what depth anomalies are real and which are not. Therefore, we can only be confident of the SeaBeam depth anomalies where we have ground-truth data, and elsewhere the results are more ambiguous. Nevertheless, the SeaBeam anomalies can still constrain the thickness, area and volume of known or suspected new lava flows at North Gorda.

5.1. The main eruption site

The results from the SeaBeam comparison show a string of large depth anomalies (Fig. 6a) located roughly along-axis within the area of the resurvey (42.45°–42.80°N). Note that Fig. 6 only shows the positive depth changes; the negative changes are omitted since we are only interested in potential additions to the crust from new lava flows. Of these anomalies, only one group is known to be associated with new lava on the seafloor (Fig. 6b), and the rest are known or presumed to be false anomalies (with one possible exception, discussed below). The large size of the false anomalies suggests that for the 1981–1996 Gorda Ridge comparison the effective detection threshold is $\sim$ 50 m, about an order of magnitude worse than on the Juan de Fuca Ridge. There is little that distinguishes the known "real" anomalies from the others. In contrast, in the SeaBeam comparison for Cleft segment, the depth anomalies due to new lava flows could be readily distinguished above the very low detection threshold (Fox et al., 1992).

The SeaBeam depth change associated with the 1996 lava flow at North Gorda is up to 75 m in the northern half, and up to 35 m in the southern half (Fig. 6b). The anomaly does not exactly match our mapped lava flow outline due to the relatively high noise level, particularly over the thinner parts of the flow. However, the thickest part of the anomaly is associated with a new ridge cutting across a formerly flat basin

in the original bathymetry, and directly overlies the steep-sided, hummocky ridge in the sidescan imagery (Fig. 5b) that is known to be 1996 lava. The area and volume of the SeaBeam anomaly (only the parts within or near the inferred flow outline) are 7.6×10^5 m^2 and 17×10^6 m^3, respectively. However, since SeaBeam anomalies only represent the thickest parts of new lava flows, this area and volume are minima. The total area of the 1996 lava flow, based on all data sources (the flow outline in Fig. 6b) is 7.9×10^5 m^2. A better estimate of the 1996 flow volume can be made by assuming a thickness of 10 m (a thickness just below the SeaBeam detection threshold) for the area of the flow "missing" from the SeaBeam anomaly. The total volume for the 1996 flow estimated by this method is 18×10^6 m^3. Revised estimates for the total volumes of lava erupted at CoAxial and Cleft on the Juan de Fuca Ridge were also made by this method and are listed in Table 1. These revised areas and volumes are considered to be more accurate than previously published values.

5.2. Was there a second eruption site?

The SeaBeam anomalies discussed above between 42.665° and 42.688°N are the only ones confirmed to be real by ground-truth data. However, there are three pieces of evidence that suggest that one of the unconfirmed anomalies might also be real. The first evidence is from the pattern of T-wave epicenters vs. time (Fox and Dziak, 1998). We speculate that the distribution of epicenters during the first half of the T-wave swarm (February 28–March 8) represents lava being erupted at the known 1996 flow site during this time; there is an initial propagation from the axial high southward, then there appears to be a clustering of epicenters between 42.6° and 42.73°N, although gaps in the SOSUS data make the pattern somewhat equivocal (see Fig. 4 of Fox and Dziak (1998)). This scenario is consistent with the fact that the *McArthur* detected event plume EP96A directly over this eruption site shortly thereafter (March 10–12); the plume appeared to be only a few days old and was almost certainly released in association with the eruption (Baker, 1998). However, in the second half of the T-wave swarm (March 10–20), the epicenters form a well-defined cluster between 42.55° and 42.65°N that is distinctly south of the known eruption site (see Fig. 4 of Fox and Dziak (1998)). A similar clustering of T-wave epicenters was also observed at the CoAxial eruption site in 1993 (Dziak et al., 1995), suggesting that eruptive activity was associated with the second half of the Gorda T-wave swarm (Fox and Dziak, 1998). One of the unconfirmed SeaBeam anomalies at 42.61°N is located in the center of this southern cluster of T-wave events (Fig. 7).

The second piece of evidence is that the SeaBeam anomaly at 42.61°N directly overlies a young, hummocky volcanic ridge in the sidescan imagery, similar in appearance to the pillow lava ridge at the known eruption site (Fig. 7). This ridge is located on the northern flank of the on-axis seamount at 42.6°N/126.823°W and extends from 42.605° to 42.615°N. The direct association of the SeaBeam anomaly with a physical feature on the seafloor which appears to be a young lava ridge, supports the idea that this unconfirmed anomaly may be real. The maximum thickness, area, and volume of the SeaBeam anomaly at 42.61°N are 60 m, 6.6×10^5 m^2, and 10×10^6 m^3, respectively (Table 1).

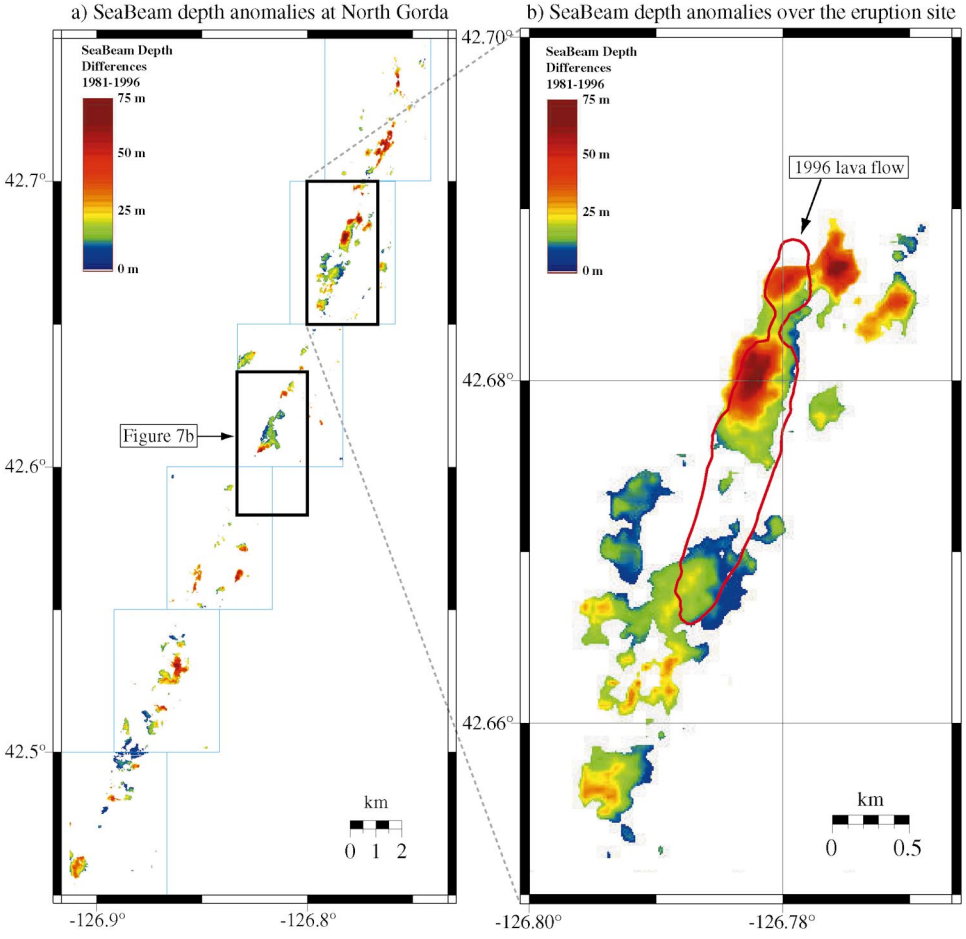

Fig. 6. Maps showing SeaBeam comparison results at North Gorda (note that only positive depth changes are shown). (a) SeaBeam depth differences between 1981 and 1996 surveys. The comparisons are done in 3′ by 3′ grids along the neovolcanic zone, shown by light blue outlines. Locations of Figs. 6b and 7b are indicated. (b) Detail of SeaBeam depth differences over the eruption site, showing 1996 lava flow (red outline). Note that thickest part of SeaBeam anomaly corresponds with steep-sided ridge in sidescan imagery (Fig. 5b).

Table 1
Estimated thicknesses, areas, and volumes of all known volcanic eruptions on the Juan de Fuca and Gorda Ridges since 1981

Eruption site	Maximum depth change from SeaBeam (m)	Area of SeaBeam anomaly ONLY ($\times 10^6$ m^2)[a]	Volume of SeaBeam anomaly ONLY ($\times 10^6$ m^3)[a]	Estimated TOTAL area of lava erupted ($\times 10^6$ m^2)[b]	Estimated TOTAL volume of lava erupted ($\times 10^6$ m^3)[c]
1996 flow (confirmed), at 42.68°N, North Gorda	75	0.76	17	0.79	18
1996 flow (unconfirmed) at 42.61°N, North Gorda	60	0.66	10	Unknown	Unknown
1993 flow, FLOW site CoAxial, JdFR	29[d]	0.36[d]	5.4[d]	0.69	8.7
1982–91 flow, FLOW site, CoAxial, JdFR	37	0.25	5.1	0.52[e]	7.8[e]
1981–91 flow, FLOC site, CoAxial, JdFR[f]	25	0.11	1.6	0.99	10
1983–87, New Pillow Mounds, North Cleft, JdFR	45	2.4	51	2.8	55

[a]Areas and volumes of SeaBeam anomalies calculated quantitatively from depth difference grids. Note, however, that these numbers are minimums since SeaBeam cannot resolve the thinnest parts of flows, which may be a substantial percentage of a flow's total area.

[b]Total flow areas estimated from mapped extent of new lava, based on near-bottom observations.

[c]Total volume of lava erupted is calculated by multiplying the "missing" area (the difference between the total flow area and the SeaBeam anomaly area) by a constant thickness of 10 m (a thickness just below the SeaBeam detection threshold) and adding this "missing" volume to the SeaBeam-anomaly volume.

[d]These numbers do not include the largest SeaBeam anomaly over the southern end of the flow, since its size was probably overestimated due to the adjacent steep slopes of Cage Volcano (see Chadwick et al. (1995)). If it *were* added, the SeaBeam-only area would be 0.46×10^6 m^2, the SeaBeam-only volume would be 8.7×10^6 m^3, and the estimated total volume of lava erupted would be 11.0×10^6 m^3.

[e]There is a little more uncertainty in the area and volume estimated for this flow than for the others because the northern extent of this eruption has not yet been determined by seafloor mapping.

[f]Note that this 1981–91 lava flow at the CoAxial FLOC site is different than the unconfirmed "southern 1981–91" anomaly discussed in Chadwick et al. (1995), which turned out to be false. The small anomaly discussed here was overlooked until camera-tow data collected in 1994 revealed a young lava flow coincident with (but much more extensive than) the anomaly. These lava flows at FLOC will be discussed in more detail in a subsequent paper.

The third piece of evidence is from the plume data. During the *Wecoma* response cruise three distinct plumes were observed at North Gorda (Baker, 1998). The first was weak and near the known eruption site, whereas the second and third plumes were larger, shallower and farther south in the axial valley and over the western wall of the valley. The helium signatures of the plumes suggest that the first and second

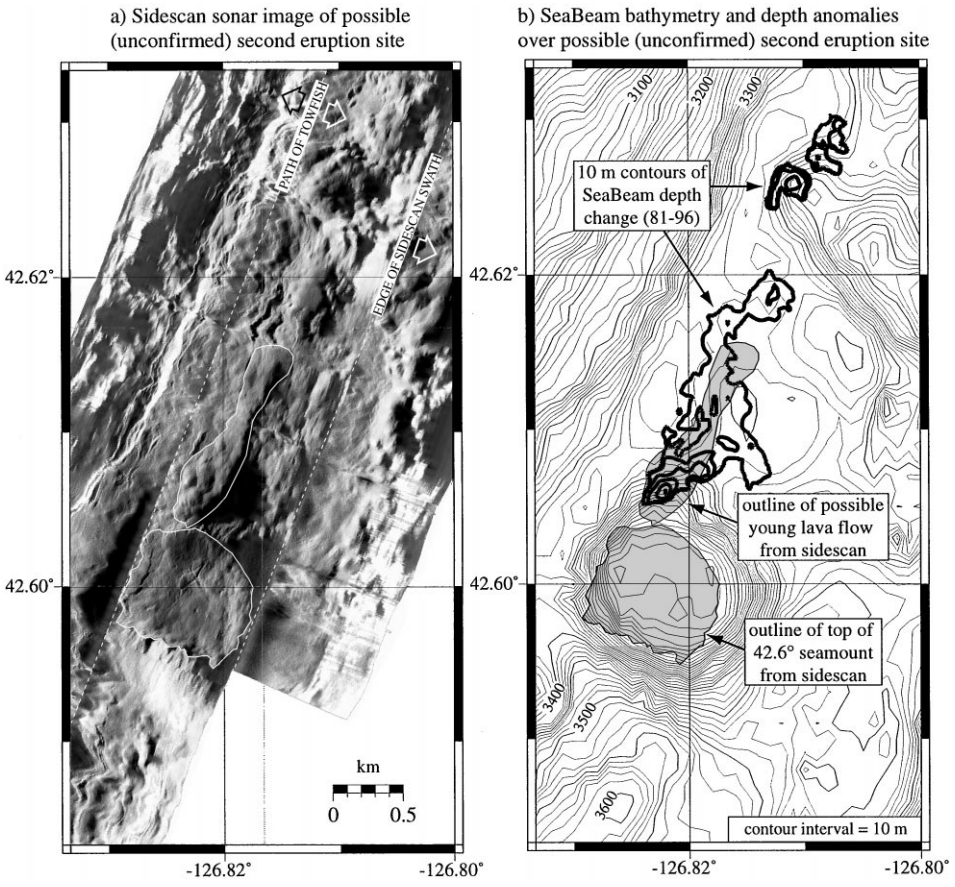

Fig. 7. (a) Sidescan sonar mosaic over possible (but unconfirmed) southern eruption site. Circular white outline at 42.6°N is the flat summit of an on-axis seamount discussed in the text, and the elongate white outline is a hummocky unfractured ridge, interpreted as a young pillow lava flow. Path of towfish and edge of overlapping swath are shown by dashed white lines. Arrows indicate the direction of insonification from the towfish. Light shades indicate high backscatter, dark shades indicate low backscatter or acoustic shadow. (b) Positive SeaBeam depth changes shown by bold contours over bathymetric map of same area (both 10 m contours). White outlines in (a) are stippled gray in (b). Largest depth change is 60 m in the southernmost part of the SeaBeam anomaly, which seems to coincide with the thickest part of the young lava flow in (a). Note that it is not known that this possible second flow was erupted in 1996.

were chronic plumes, but the third was an event plume, EP96B (Baker, 1998). Baker (1998) interpret that both the second and third plumes may have originated from the hypothetical second eruption site at 42.61°N, because they were unconnected with the plume from the known eruption site, no plume signals were found from this area of the segment during the *McArthur* cruise (before the second T-wave swarm had started), and the plumes differ in their chemistry (Cowen et al., 1998; Feely et al., 1998; Massoth et al., 1998). Baker (1998) also conclude that event plume EP96A is different

from EP96B because they differ strongly in their total heat, plume temperature maxima, and chemistry (Cowen et al., 1998; Feely et al., 1998; Massoth et al., 1998), suggesting that there had to be at least two separate event plume forming events (eruptions or intrusions).

Together, these three lines of evidence show that it is possible (but not proven) that there were two eruption sites associated with the 1996 eruption—one at 42.665°–42.688°N and the other at 42.605°–42.615°N. The distribution of our camera data is limited to the northern eruption site (collected in only 2 days made available on the *Wecoma*), and no bottom photography exists over the southern site. Obviously, it is important to collect seafloor imagery as soon as possible over this southern site to determine whether or not lava actually erupted here in 1996. Another possibility is that an eruption occurred here between the 1981 and 1996 SeaBeam surveys, but before the 1996 events. Collecting the bottom photography necessary to resolve this question would tell us the true volume of the 1996 eruption, the full extent of the segment that was volcanically active during this event, and would help in the interpretation of other datasets collected during the event response.

6. Discussion: lessons for future event responses

(1) Visual imagery of the seafloor is critical for determining whether lava erupted during an event response, and for defining the location, extent, and the character of the event. A towed camera system (or an ROV, if available) is required to collect this imagery over significant areas, and must be in a near-ready state to be able to participate in an event response at short notice. Some kind of temperature sensor on the camera sled is also extremely useful, since newly erupted flows are still hot and cooling. Systems capable of real-time data transmission are highly desirable. Acoustic transponders are also desirable for providing accurate navigation, but also require extra time to deploy, calibrate, and recover.

(2) This is the second time that a new lava flow was found directly under a newly formed event plume (the other example being the CoAxial eruption (Embley et al., 1995b)). The North Gorda eruption further establishes the causal link between eruption sites and event plume formation (Lowell and Germanovich, 1995; Baker, 1998). It also indicates that if an event plume is found early enough during a rapid response (within days or weeks of its formation before it has drifted from its point of origin), then its location is the best place to start looking for a new eruption site on the seafloor. This may be especially helpful in future event responses since T-wave epicenters may be distributed over 10's of km of ridge crest and may not necessarily localize at an eruption site (Fox and Dziak, 1998).

(3) SeaBeam comparisons are severely limited if the navigation from the earlier survey is poor. Therefore, in areas where detectable eruptions are likely and only poorly navigated (pre-1992) multibeam surveys exist, these areas should be resurveyed with GPS-navigated multibeam to establish a high-quality bathymetric baseline, so that any future comparisons will be more definitive. For example, we plan to complete a resurvey of the neovolcanic zone of the entire Gorda Ridge in the near future

(Bobbitt et al., 1997). During an event response, time should be taken to collect a proper repeat survey (not just during other operations). The aim when collecting the repeat survey is to minimize any differences between the before and after surveys, so that the comparison can distinguish areas with real change from those areas with no change. Achieving a good signal to noise ratio in the comparisons can only be accomplished if the repeat surveys are collected carefully and if possible with the same multibeam system, along the same tracklines, and at the same ship speed. The more dissimilar the before and after surveys are, the more noise gets introduced into the comparison, until eventually a useful comparison is no longer possible.

(4) SeaBeam data should be collected as early as possible in a rapid response, because it can help tell where a new lava flow is or might be, where the thickest flows are located, etc., and this information is vital for many other response investigations. For example, in the Gorda response, a SeaBeam resurvey was not completed until 4 months after the eruption, and by that time it was too late to take advantage of the results for the towed-camera and *ATV* surveys, and the potential second lava flow was unknown so no seafloor imagery was collected there to determine if the eruption really extended this far south or not. In addition, if the *McArthur* could have collected multibeam data when it first got to the site, it is possible that it could have unequivocally documented and constrained the exact timing of the southern lava flow, since *McArthur* was there while the southern T-wave swarm (and possibly the southern eruption) was just starting.

7. Conclusions

The combination of camera, ROV, sidescan, and SeaBeam data provides a more comprehensive view of the 1996 lava flow at North Gorda than would be possible from any of these data sources alone. We have used these data to map the flow's outline (Figs. 2, 5, and 6), which is 2.6 km long, 400 m wide, 1.5×10^6 m^2 in area, and extends from 42.665° to 42.688°N. The SeaBeam data shows that the flow is up to 75 m thick and we estimate the erupted volume to be 18×10^6 m^3. The 1996 lava flow is similar in morphology to the other recently erupted pillow-lava flows on the Juan de Fuca Ridge, and is clearly the product of a fissure eruption where a dike reached the surface. The northern half of the flow is much thicker than the southern half, indicating that the northern part of the eruptive fissure was much longer-lived than the rest. This is consistent with observations on land, where dike-fed fissure eruptions commonly localize to a few discrete vents after an initial "curtain of fire" stage (Bruce and Huppert, 1989). Eruptive localization was also evident for the mid-1980s Cleft eruption, where 80% of the lava was emplaced at the distal end of the 17 km long eruptive fissure (Chadwick and Embley, 1994). The Gorda flow is thicker and steeper-sided than the other recent flows at Cleft and CoAxial, but is intermediate in volume (Table 1). Despite its seemingly impressive size, the 1996 flow is relatively small (perhaps 10%) compared to the older pillow ridges imaged by sidescan sonar on the North Gorda segment (Fig. 5), suggesting that much larger eruptions are possible.

A combination of evidence from T-wave, plume, sidescan, and SeaBeam data suggest that there may have been a second eruption site between 42.605° to 42.615°N, about 8 km south of the known 1996 lava flow. However, this interpretation remains speculative and unconfirmed due to the lack of near-bottom imagery over this site.

Acknowledgements

Special thanks to the people who were critical to making the camera tows on the *Wecoma* successful: NSF/RIDGE for funding the *Wecoma* response cruise, Dan Fornari, who helped ensure that the WHOI camera sled was available and ready on very short notice, Earl Young, who kept the ornery camera system operational at sea, Susan Hanneman, who helped operate the camera system and develop film at sea, and Marc Willis and the crew of the *Wecoma* who skillfully facilitated our towing operations in challenging conditions. Another set of people deserve special thanks for their support during the AMS-60 sidescan sonar operations on the *Discoverer*: Nick Lesnikowski and the other sidescan operators from Williamson and Associates, and Stuart Sides and Miguel Velasco from the U.S. Geological Survey, who processed the sidescan data at sea, and the captain and crew of the *Discoverer*, who helped us collect the data smoothly and efficiently on her final cruise. Thanks also to Ed Baker for collecting the SeaBeam data on the *Discoverer* in June, and to H. Paul Johnson for sharing his observational data from *Jason* dive 191. Funding for *ATV* dive 178 at Gorda Ridge was supported by NOAA's West Coast Undersea Research Center (WCNURC) and the U.S. Navy. This research was partially funded by the NOAA/VENTS Program. PMEL contribution #1875.

References

Baker, E.T., Massoth, G.J., Collier, R.W., Trefry, J.H., Kadko, D., Nelsen, T.A., Rona, P.A., Lupton, J.E., 1987. Evidence for high-temperature venting on the Gorda Ridge, northeast Pacific Ocean. Deep-Sea Research II 34, 1461–1476.

Baker, E.T., Massoth, G.J., Feely, R.A., Embley, R.W., Thomson, R.E., Burd, B.J., 1995. Hydrothermal event plumes from the CoAxial seafloor eruption site, Juan de Fuca Ridge. Geophysical Research Letters 22, 147–150.

Baker, E.T., 1998. Patterns of event and chronic hydrothermal venting following a magmatic intrusion: New perspectives from the 1996 Gorda Ridge eruption. Deep-Sea Research II 45, 2599–2618.

Ballard, R.D., van Andel, T.H., 1977. Morphology and tectonics of the inner rift valley at 36°50′N on the Mid-Atlantic Ridge. Geological Society of America Bulletin 88, 507–530.

Bobbitt, A.M., Dziak, R.P., Fox, C.G., 1997. High-resolution bathymetric mapping of an entire tectonic plate: Gorda Plate, northeast Pacific Ocean. EOS Transactions of the American Geophysical Union 78, 46 (Fall Meeting Suppl.), F630.

Bruce, P.M., Huppert, H.E., 1989. Thermal control of basaltic fissure eruptions. Nature 342, 665–667.

Chadwick, Jr, W.W., Embley, R.W., 1994. Lava flows from a mid-1980s submarine eruption on the Cleft Segment, Juan de Fuca Ridge. Journal of Geophysical Research 99, 4761–4776.

Chadwick, Jr, W.W., Embley, R.W., 1998. Graben formation associated with recent dike intrusions and volcanic eruptions on the mid-ocean ridge. Journal of Geophysical Research 103, 9807–9825.

Chadwick, Jr, W.W., Embley, R.W., Fox, C.G., 1991. Evidence for volcanic eruption on the southern Juan de Fuca Ridge between 1981 and 1987. Nature 350, 416–418.

Chadwick, Jr, W.W., Embley, R.W., Fox, C.G., 1995. SeaBeam depth changes associated with recent lava flows, CoAxial segment, Juan de Fuca Ridge: Evidence for multiple eruptions between 1981–1993. Geophysical Research Letters 22, 167–170.

Chadwick, Jr, W.W., Embley, R.W., Johnson, P.D., 1996. Comparative study of recent eruptive sites on the Gorda and Juan de Fuca Ridges using AMS-60 sidescan sonar. EOS Transactions of the American Geophysical Union 77, 46 (Fall Meeting Suppl.), F1.

Clague, D.A., Holmes, M.L., 1987. Geology, petrology, and mineral potential of the Gorda Ridge. In: Scholl, D.W., Grantz, A., Vedder, J. (Eds.), Geology and Resource Potential of the Continental Margin of Western North America and Adjacent Ocean Basins—Beaufort Sea to Baja California. Circum-Pacific Council for Energy and Mineral Resources, Earth Science Series, Vol. 6. American Association of Petroleum Geologists, Houston, pp. 563–580.

Clague, D.A., Rona, P.A., 1990. Geology of the GR14 site on the Northern Gorda Ridge. In: McMurray, G.R. (Ed.), Gorda Ridge: A Seafloor Spreading Center in the U.S. Exclusive Economic Zone. Springer, New York, pp. 31–50.

Cochran, J.R. et al., 1997. The Southeast Indian Ridge between 88°E and 118°E: gravity anomalies and crustal accretion at intermediate spreading rates. Journal of Geophysical Research 102, 15 463–15 487.

Collier, R.W., Baker, E.T., 1990. Hydrography and geochemistry of northern Gorda Ridge. In: McMurray, G.R. (Ed.), Gorda Ridge: A Seafloor Spreading Center in the U.S. Exclusive Economic Zone. Springer, New York, pp. 21–30.

Cowen, J.P., Bertram, M.A., Baker, E.T., Feely, R.A., Massoth, G.J., Summit, M., 1998. Geomicrobial transformation of manganese in Gorda Ridge event plumes. Deep-Sea Research II 45, 2713–2737.

Crane, K., Ballard, R.D., 1981. Volcanics and structure of the Famous Narrowgate Rift: evidence for cyclic evolution: AMAR 1. Journal of Geophysical Research 86, 5112–5124.

Dziak, R.P., Fox, C.G., Schreiner, A.E., 1995. The June–July 1993 seismo-acoustic event at CoAxial segment, Juan de Fuca Ridge: evidence for a lateral dike injection. Geophysical Research Letters 22, 135–138.

Embley, R.W., Chadwick Jr, W.W., 1994. Volcanic and hydrothermal processes associated with a recent phase of seafloor spreading at the northern Cleft segment: Juan de Fuca Ridge. Journal of Geophysical Research 99, 4741–4760.

Embley, R.W., Chadwick Jr, W.W., Getsiv, J., 1995a. The CoAxial segment: A site of recent seafloor eruptions on the Juan de Fuca Ridge. EOS Transactions of the American Geophysical Union 76, 46 (Fall Meeting Suppl.), F410.

Embley, R.W., Chadwick Jr, W.W., Jonasson, I.R., Butterfield, D.A., Baker, E.T., 1995b. Initial results of the rapid response to the 1993 CoAxial event: relationships between hydrothermal and volcanic processes. Geophysical Research Letters 22, 143–146.

Embley, R.W., Chadwick Jr, W.W., Perfit, M.R., Baker, E.T., 1991. Geology of the northern Cleft segment, Juan de Fuca Ridge: Recent lava flows, sea-floor spreading, and the formation of megaplumes. Geology 19, 771–775.

Embley, R.W., Chadwick Jr, W.W., Shank, T., Christie, D., 1996. Geology of the 1996 Gorda Ridge eruption from analysis of multibeam, towed camera, sidescan, and ROV data. EOS Transactions American Geophysical Union 77, 46 (Fall Meeting Suppl.), F1.

Feely, R.A., Baker, E.T., Lebon, G.T., Gendron, J.F., Massoth, G.J., Mordy, C.W., 1998. Chemical variations of hydrothermal particles in the 1996 Gorda Ridge event and chronic plumes. Deep-Sea Research II 45, 2637–2664.

Fox, C.G., Chadwick Jr, W.W., Embley, R.W., 1992. Detection of changes in ridge-crest morphology using repeated multibeam sonar surveys. Journal of Geophysical Research 97, 11 149–11 162.

Fox, C.G., Dziak, R.P., 1998. Hydroacoustic detection of volcanic activity on the Gorda Ridge, February–March 1996. Deep-Sea Research II 45, 2513–2530.

Fox, C.G., Dziak, R.P., Matsumoto, H., Schreiner, A.E., 1994. Potential for monitoring low-level seismicity on the Juan de Fuca Ridge using military hydrophone arrays. Marine Technology Society Journal 27, 22–30.

Fox, C.G., Radford, W.E., Dziak, R.P., Lau, T.K., Matsumoto, H., Schreiner, A.E., 1995. Acoustic detection of a seafloor spreading episode on the Juan de Fuca Ridge using military hydrophone arrays. Geophysical Research Letters 22, 131–134.

Fox, P.J., Grindlay, N.R., Macdonald, K.C., 1991. The Mid-Atlantic Ridge (31°S–34°30′S): Temporal and spatial variations of accretionary processes. Marine Geophysical Researches 13, 1–20.

Fujimoto, H., Seama, N., Lin, J., Matsumoto, T., Tanaka, T., Fujioka, K., 1996. Gravity anomalies of the Mid-Atlantic Ridge north of the Kane Fracture Zone. Geophysical Research Letters 23, 3431–3434.

Gregg, T.K.P., Fink, J.H., 1995. Quantification of submarine lava-flow morphology through analog experiments. Geology 23, 73–76.

Griffiths, R.W., Fink, J.H., 1992. Solidification and morphology of submarine lavas: a dependence on extrusion rate. Journal of Geophysical Research 97, 19 729–19 737.

Grim, M.S., Chase, T.E., Evenden, G.I., Holmes, M.L., Normark, W.R., Wilde, P., Fox, C.G., Lief, C.J., Seekins, B.A., 1992. Map showing bottom topography of the Pacific continental margin, Strait of Juan de Fuca to Cape Mendocino. Miscellaneous Investigation Series, Map I-2091-C, U.S. Geological Survey.

Grindlay, N.R., Fox, P.J., Macdonald, K.C., 1991. Second-order ridge axis discontinuities in the south Atlantic: Morphology, structure and evolution. Marine Geophysical Researches 13, 21–49.

Head, J.W., Wilson, L., Smith, D.K., 1996. Mid-ocean ridge eruptive vents: Evidence for dike widths, eruption rates, and evolution of eruptions from morphology and structure. Journal of Geophysical Research 101, 28 265–28 280.

Hooft, E.E.E., Detrick, R.S., 1995. Relationship between axial morphology, crustal thickness, and mantle temperature along the Juan de Fuca and Gorda Ridges. Journal of Geophysical Research 100, 22 499–22 508.

Howard, K.J., Fisk, M.R., 1988. Hydrothermal alumina-rich clays and boehmite on the Gorda Ridge. Geochimica et Cosmochimica Acta 52, 2269–2279.

Johnson, H.P., Hutnak, M., 1997. Conductive heat loss in recent eruptions at mid-ocean ridges. Geophysical Research Letters 24, 3089–3092.

Kuo, B.Y., Forsyth, D.W., 1988. Gravity anomalies of the ridge-transform system in the south Atlantic between 31 and 34.5°S: upwelling centers and variation in crustal thickness. Marine Geophysical Researches 10, 205–232.

Lin, J., Purdy, G.M., Schouten, H., Sempéré, J.C., Zervas, C., 1990. Evidence from gravity data for focused magmatic accretion along the Mid-Atlantic Ridge. Nature 344, 627–632.

Lowell, R.P., Germanovich, L.N., 1995. Dike injection and the formation of megaplumes at ocean ridges. Science 267, 1804–1807.

Lupton, J.E., Baker, E.T., Garfield, N., Massoth, G., Feely, R., Greene, R., Rago, T., 1998. Tracking the evolution of a hydrothermal event plume using a RAFOS neutrally buoyant drifter. Science 280, 1052–1055.

Masson, D.G., Cacchione, D.A., Drake, D.E., 1988. Tectonic evolution of Gorda Ridge inferred from sidescan sonar images. Marine Geophysical Researches 10, 191–204.

Massoth, G.J., Baker, E.T., Feely, R.A., Lupton, J.E., Collier, R.W., Gendron, J.F., Roe, R.K., Maenner, S.M., Resing, J.A., 1998. Manganese and iron in hydrothermal plumes resulting from the 1996 Gorda Ridge Event. Deep-Sea Research II 45, 2683–2712.

Parsons, T., Thompson, G.A., 1991. The role of magma overpressure in suppressing earthquakes and topography: Worldwide examples. Science 253, 1399–1402.

Phipps Morgan, J., Chen, Y.J., 1993. Dependence of ridge-axis morphology on magma supply and spreading rate. Nature 364, 706–708.

Phipps Morgan, J., Parmentier, E.M., Lin, J., 1987. Mechanisms for the origin of mid-ocean ridge axial topography: implications for the thermal and mechanical structure of accreting plate boundaries. Journal of Geophysical Research 92, 12 823–12 836.

Riddihough, R., 1980. Gorda plate motions from magnetic anomaly analysis. Earth and Planetary Science Letters 51, 163–170.

Rona, P.A., Beaverson, C.A., Fox, C.G., Embley, R.W., Hammond, S.R., 1992. Geologic setting of hydrothermal activity at the Gorda Ridge. EOS Transactions American Geophysical Union 73, 43 (Fall Meeting Suppl.), 254.

Rona, P.A., Clague, D.A., 1989. Geologic controls of hydrothermal discharge on the northern Gorda Ridge. Geology 17, 1097–1101.

Rona, P.A., Denlinger, R.P., Fisk, M.R., Howard, K.J., Taghon, G.L., Klitgord, K.D., McClain, J.S., McMurray, G.R., Wiltshire, J.C., 1990. Major off-axis hydrothermal activity on the northern Gorda Ridge. Geology 18, 493–496.

Rubin, K.H., Smith, M.C., Perfit, M.R., Christie, D.M., Sacks, L.F., 1998. Geochronology and geochemistry of lavas from the 1996 North Gorda Ridge eruption. Deep-Sea Research II 45, 2571–2597.

Sempéré, J.C. et al. 1997. The Southeast Indian Ridge between 88°E and 118°E: variations in crustal accretion at constant spreading rate. Journal of Geophysical Research 102, 15 489–15 505.

Sempéré, J.C., Lin, J., Brown, H.S., Schouten, H., Purdy, G.M., 1993. Segmentation and morphotectonic variations along a slow-spreading center: the Mid-Atlantic Ridge (24°00′N–30°40′N). Marine Geophysical Researches 15, 153–200.

Sempéré, J.C., Palmer, J., Christie, D., Phipps Morgan, J., Shor, A., 1991. Australian–Antarctic discordance. Geology 19, 429–432.

Sempéré, J.C., West, B.P., Géli, L., 1996. The Southeast Indian Ridge between 127° and 132°40′E: Contrasts in segmentation characteristics and implications for crustal accretion. In: MacLead, C.J., Tyler, P., Walker, C.L., (Eds.), Tectonic, Magmatic, Hydrothermal and Biological Segmentation of Mid-Ocean Ridges, Special Publication 118. Geological Society of London, pp. 1–15.

Smith, D.K., 1996. Comparison of the shapes and sizes of seafloor volcanoes on Earth and "pancake" domes on Venus. Journal of Volcanology and Geothermal Research 73, 47–64.

Smith, D.K., et al., 1995. Mid-Atlantic Ridge volcanism from deep-towed side-scan sonar images, 25°–29°N. Journal of Volcanology and Geothermal Research 67, 233–262.

Tivey, M.A., 1994. Fine-scale magnetic anomaly field over the southern Juan de Fuca Ridge: Axial magnetization low and implications for crustal structure. Journal of Geophysical Research 99, 4833–4855.

Wilson, D.S., 1986. A kinematic model for the Gorda deformation zone as a diffuse southern boundary of the Juan de Fuca plate. Journal of Geophysical Research 91, 10 259–10 269.

Wilson, D.S., 1989. Deformation of the so-called Gorda Plate. Journal of Geophysical Research 94, 3065–3075.